# Hybrid bioinorganic approach to solar-to-chemical conversion

Eva M. Nichols[a,b,1], Joseph J. Gallagher[c,1], Chong Liu[a,d], Yude Su[a], Joaquin Resasco[e], Yi Yu[a], Yujie Sun[f], Peidong Yang[a,d,g,h,2], Michelle C. Y. Chang[a,b,c,2], and Christopher J. Chang[a,b,c,i,2]

[a]Department of Chemistry, University of California, Berkeley, CA 94720; [b]Chemical Sciences Division, Lawrence Berkeley National Laboratory, Berkeley, CA 94720; [c]Department of Molecular and Cell Biology, University of California, Berkeley, CA 94720; [d]Materials Sciences Division, Lawrence Berkeley National Laboratory, Berkeley, CA 94720; [e]Department of Chemical Engineering, University of California, Berkeley, CA 94720; [f]Department of Chemistry and Biochemistry, Utah State University, Logan, UT 84322; [g]Department of Materials Science and Engineering, University of California, Berkeley, CA 94720; [h]Kavli Energy NanoSciences Institute, Berkeley, CA 94720; and [i]Howard Hughes Medical Institute, University of California, Berkeley, CA 94720

Edited by Richard Eisenberg, University of Rochester, Rochester, New York, and approved July 24, 2015 (received for review April 26, 2015)

**Natural photosynthesis harnesses solar energy to convert $CO_2$ and water to value-added chemical products for sustaining life. We present a hybrid bioinorganic approach to solar-to-chemical conversion in which sustainable electrical and/or solar input drives production of hydrogen from water splitting using biocompatible inorganic catalysts. The hydrogen is then used by living cells as a source of reducing equivalents for conversion of $CO_2$ to the value-added chemical product methane. Using platinum or an earth-abundant substitute, α-NiS, as biocompatible hydrogen evolution reaction (HER) electrocatalysts and *Methanosarcina barkeri* as a biocatalyst for $CO_2$ fixation, we demonstrate robust and efficient electrochemical $CO_2$ to $CH_4$ conversion at up to 86% overall Faradaic efficiency for ≥7 d. Introduction of indium phosphide photocathodes and titanium dioxide photoanodes affords a fully solar-driven system for methane generation from water and $CO_2$, establishing that compatible inorganic and biological components can synergistically couple light-harvesting and catalytic functions for solar-to-chemical conversion.**

artificial photosynthesis | solar fuels | photocatalysis | carbon dioxide fixation | water splitting

Methods for the sustainable conversion of carbon dioxide to value-added chemical products are of technological and societal importance (1–3). Elegant advances in traditional approaches to $CO_2$ reduction driven by electrical and/or solar inputs using homogeneous (4–16), heterogeneous (17–26), and biological (7, 27–31) catalysts point out key challenges in this area, namely (*i*) the chemoselective conversion of $CO_2$ to a single product while minimizing the competitive reduction of protons to hydrogen, (*ii*) long-term stability under environmentally friendly aqueous conditions, and (*iii*) unassisted light-driven $CO_2$ reduction that does not require external electrical bias and/or sacrificial chemical quenchers. Indeed, synthetic homogeneous and heterogeneous $CO_2$ catalysts are often limited by product selectivity and/or aqueous compatibility, whereas enzymes show exquisite specificity but are generally less robust outside of their protective cellular environment. In addition, the conversion of electrosynthetic systems to photosynthetic ones is nontrivial owing to the complexities of effectively integrating components of light capture with bond-making and bond-breaking chemistry.

Inspired by the process of natural photosynthesis in which light-harvesting, charge-transfer, and catalytic functions are integrated to achieve solar-driven $CO_2$ fixation (32–35), we have initiated a program in solar-to-chemical conversion to harness the strengths inherent to both inorganic materials chemistry and biology (36). As shown in Fig. 1, our strategy to drive synthesis with sustainable electrical and/or solar energy input (37) interfaces a biocompatible photo(electro)chemical hydrogen evolution reaction (HER) catalyst with a microorganism that uses this sustainably generated hydrogen as an electron donor for $CO_2$ reduction. Important previous reports have shown the feasibility of electrosynthesis (38–42) but have not yet established solar-driven processes. We selected methane as an initial target for this approach owing to the ease of product separation, the potential for integration into existing infrastructures for the delivery and use of natural gas (of which $CH_4$ is the principle component), and the fact that direct conversion of $CO_2$ to $CH_4$ with synthetic catalysts remains a formidable challenge due to large overpotentials and poor $CH_4/H_2$ selectivity. Two of the most active and selective direct electrocatalysts for $CO_2$ to $CH_4$ conversion reported to date produce methane with 61% (43) and 76% (44) Faradaic efficiencies, but require overpotentials of $\eta = 1.28$ V and $\eta = 1.52$ V, respectively. Promising advances in photothermal reduction of $CO_2$ to $CH_4$ also have been recently reported (45). In comparison with fully inorganic catalysts, a distinct conceptual advantage of this hybrid materials biology approach, where the materials component performs water splitting to generate hydrogen and the biological component uses these reducing equivalents for $CO_2$ fixation, is that one can leverage the fact that biological catalysts operate at near thermodynamic potential (46). As such, the only overpotential involved is associated with hydrogen evolution from water, a more facile reaction to catalyze via sustainable electrochemical and photochemical means compared with $CO_2$ reduction. Coupled with the diversity of potential chemical products available via synthetic biology, the marriage between artificial and natural platforms can create opportunities to develop catalyst systems with enhanced function over the individual parts in isolation.

In developing hybrid bioinorganic platforms for solar-to-chemical conversion of $CO_2$, we drew inspiration from both

## Significance

Natural photosynthesis, a process of solar-to-chemical conversion, uses light, water, and carbon dioxide to generate the chemical products needed to sustain life. Here we report a strategy inspired by photosynthesis in which compatible inorganic and biological components are used to transform light, water, and carbon dioxide to the value-added product methane. Specifically, this solar-to-chemical conversion platform interfaces photoactive inorganic materials that produce hydrogen from water and sunlight with microorganisms that consume this sustainably derived hydrogen to drive the transformation of carbon dioxide to methane with high efficiency. This system establishes a starting point for a broader materials biology approach to the synthesis of more complex chemical products from carbon dioxide and water.

Author contributions: E.M.N., J.J.G., C.L., P.Y., M.C.Y.C., and C.J.C. designed research; E.M.N., J.J.G., C.L., Y. Su, J.R., Y.Y., and Y. Sun performed research; E.M.N., J.J.G., C.L., P.Y., M.C.Y.C., and C.J.C. analyzed data; and E.M.N., J.J.G., C.L., P.Y., M.C.Y.C., and C.J.C. wrote the paper.

The authors declare no conflict of interest.

This article is a PNAS Direct Submission.

[1]E.M.N. and J.J.G. contributed equally to this work.

[2]To whom correspondence may be addressed. Email: p_yang@berkeley.edu, mcchang@berkeley.edu, or chrischang@berkeley.edu.

This article contains supporting information online at www.pnas.org/lookup/suppl/doi:10.1073/pnas.1508075112/-/DCSupplemental.

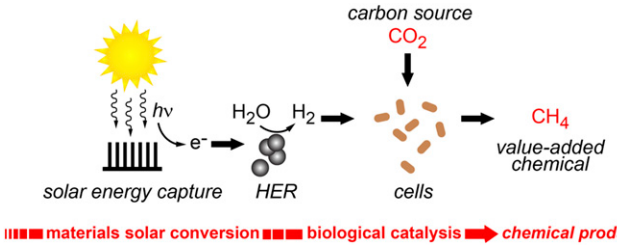


**Fig. 1.** General scheme depicting a hybrid bioinorganic approach to solar-to-chemical conversion. Sustainable energy inputs in the form of electrical potential or light can be used to generate hydrogen from water using inorganic HER catalysts; biological hydrogen-driven $CO_2$ fixation can subsequently generate value-added products such as methane. This materials biology interface can be generalized to other chemical intermediates and end products by mixing and matching different compatible inorganic and biological components.

tandem organometallic–microbial systems (47, 48), in which products of microbial metabolism are further transformed by organometallic catalysts, as well as biological electrosynthesis, in which organisms accept reducing equivalents from an electrode either in the form of soluble electron carriers (for example, $H_2$ or formate) (41, 49, 50) or via direct electron transfer (36, 51–53). Engineered strains of *Ralstonia eutropha* have been used for the aerobic production of isobutanol and 3-methyl-1-butanol (41), and isopropanol (42). However, owing to the oxygen requirements of this organism and the relative inefficiency of its carbon fixation pathways (54), product titers and production efficiencies are relatively modest, and generation of reactive oxygen species is a serious concern. In addition, to our knowledge, no photosynthetic systems of this type have been reported. As such, we turned our attention to the use of a pure culture of *Methanosarcina barkeri*, an obligately anaerobic archaeon that fuels its metabolism via the 8-proton, 8-electron reduction of $CO_2$ to $CH_4$ (55). Prior studies have reported methanogenic electrosynthesis (51, 53, 56); however, a fully light-driven system remains to be realized. Additionally, mixed cultures and multiple possible sources of reducing equivalents have complicated Faradaic efficiency measurements in previous studies (51, 53, 56). Through the design of our hybrid system, we sought to surmount some of these aforementioned challenges.

Here we report an integrated bioinorganic catalyst platform for solar-to-chemical $CO_2$ conversion using sustainable inorganic hydrogen generators in conjunction with $CO_2$-fixing archaea. Under electrosynthetic conditions with a platinum cathode, a culture of *M. barkeri* shows chemoselective conversion of $CO_2$ to $CH_4$ with high Faradaic efficiencies (up to 86%) and low overpotential ($\eta$ = 360 mV). The system is also capable of high yield production, cumulatively generating 110 mL (4.3 mmol) of methane over 7 d. Isotope labeling with $^{13}CO_2$ establishes that $CH_4$ is uniquely derived from $CO_2$ for cultures in both rich media and minimal, carbon-free media. Replacement of Pt with an earth-abundant α-NiS electrocatalyst allows for $CH_4$ generation at similar titers. Moreover, using a photoactive silicon cathode reduces the overpotential to 175 mV upon irradiation with 740-nm light. Unassisted light-driven methane generation was achieved using tandem solar absorption by a photoactive *n*-$TiO_2$ anode and *p*-InP cathode assembly. Taken together, the results demonstrate the feasibility of combining compatible inorganic and biological systems to achieve solar-to-chemical conversion from light, $H_2O$, and $CO_2$, affording a starting point for the realization of sustainable fixation of $CO_2$ to value-added molecules.

## Results and Discussion

**Selection of Biological Catalyst.** Careful organism selection is critical to the successful realization of an integrated bioinorganic system. The autotrophic obligate anaerobe *M. barkeri* (55) is amenable to integration with inorganic catalysts for a variety of reasons. *M. barkeri* can use $H_2$ as a source of reducing equivalents for the reduction of $CO_2$ to $CH_4$; the cathode of a water-splitting device could serve as a potential source of this $H_2$. Owing to the anaerobic metabolism of the organism, oxygen is not required at the cathode, thereby improving Faradaic efficiency for the product of interest, simplifying gas delivery to the culture, and preventing generation of potentially harmful reactive oxygen species. Furthermore, $CH_4$ is generated with high efficiency as a byproduct of normal metabolism. Finally, *M. barkeri* requires no added sources of reduced carbon and can produce $CH_4$ in minimal media containing only supplemental vitamins and minerals.

**Electrochemical Reduction of Carbon Dioxide to Methane with a Hybrid Platinum/Archaea Catalyst Platform.** Initial experiments were performed using a platinum cathode to electrochemically generate $H_2$, which was subsequently used in situ by *M. barkeri* to reduce $CO_2$ to $CH_4$. Fig. 2*A* shows a general schematic of the gas-tight, two-compartment electrochemical cell that was specially fabricated for batch-mode electrolysis and subsequent headspace analysis by gas chromatography (GC). (See Fig. S1 for electrolysis cell photo.) Separation of the cathodic and anodic chambers with an ion-permeable membrane prevented any noticeable diffusion of $O_2$ into the culture. After inoculation of the cathodic chamber with *M. barkeri* (130-mL final volume, $OD_{600\ nm}$ = 0.35) and saturation of the carbon-free catholyte with pure $CO_2$,

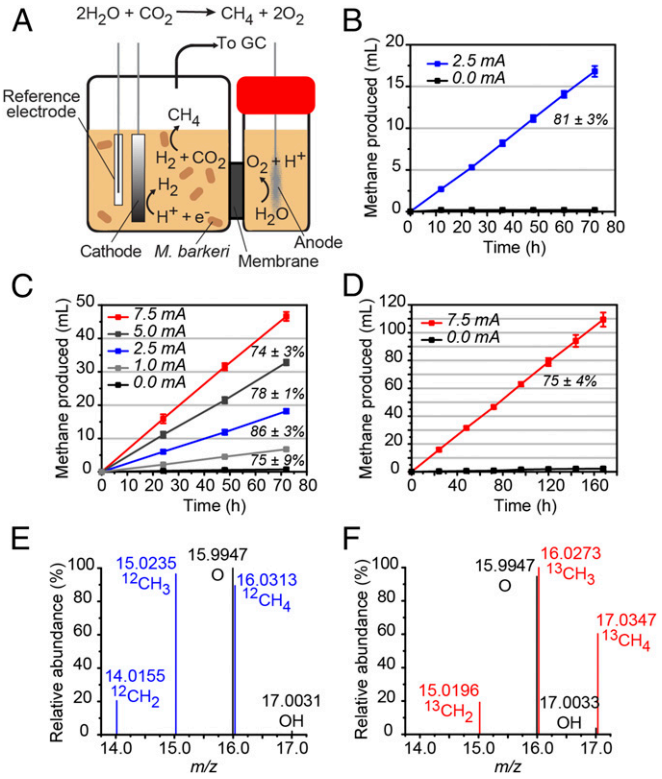


**Fig. 2.** Electrocatalytic reduction of carbon dioxide to methane with a hybrid platinum/*M. barkeri* platform. (*A*) Schematic of generalized electrolytic setup showing in situ generation of hydrogen at the cathode followed by hydrogen-driven reduction of carbon dioxide to methane by the *M. barkeri* biocatalyst. (*B*) Cumulative methane generation and associated average Faradaic efficiency in minimal media. (*C*) Cumulative methane generation and associated average Faradaic efficiencies at various currents in rich media. (*D*) Cumulative long-term methane generation and associated average Faradaic efficiency in rich media. (*E* and *F*) High-resolution mass spectrometry of headspace gases after electrolysis under an atmosphere of (*E*) $^{12}CO_2$ and (*F*) $^{13}CO_2$ in rich media. Error bars represent SD with $n$ = 3 independent experiments in all cases.

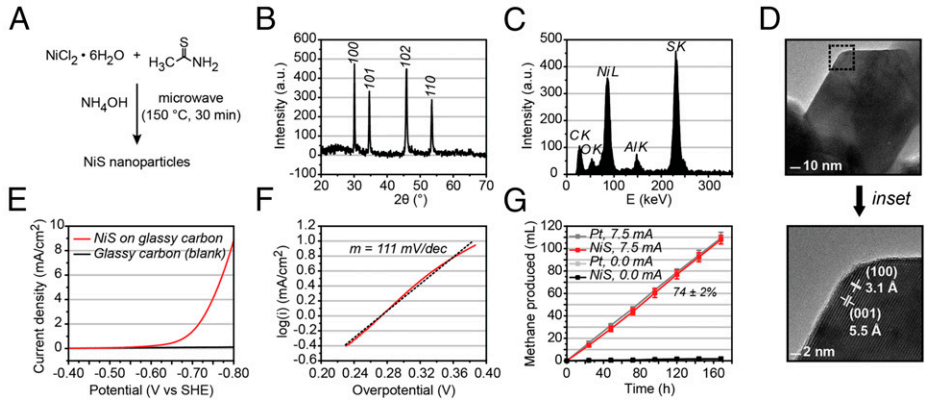


**Fig. 3.** Synthesis and characterization of a biocompatible, earth-abundant HER catalyst for use in hybrid bioinorganic systems. (*A*) Synthesis of α-NiS nanoparticles. (*B*) pXRD pattern of α-NiS. (*C*) EDX spectrum of α-NiS. (*D*) HRTEM images of α-NiS. (*E*) Polarization curve (RDE) of α-NiS on glassy carbon compared with glassy carbon background, 1 M $KP_i$ (pH 7), scan rate 5 mV/s, rotation speed 1,500 rpm. (*F*) Corresponding Tafel plot. (*G*) Cumulative long-term methane generation and associated average Faradaic efficiency using an α-NiS/carbon cloth cathode is comparable to results obtained with platinum cathodes. Error bars represent SD with $n = 3$ independent experiments.

galvanostatic electrolysis was performed at a current of 2.5 mA ($j = 0.29$ mA/cm$^2$, $\eta = 360$ mV) for 11.5 h, followed by 0.5 h of sampling. (See the *Supporting Information* for calculation of overpotentials.) The headspace was analyzed by GC and replaced by sparging with fresh $CO_2$ before restarting the electrolysis. (See Fig. S2 for GC calibration curves.) Methane production was linear under these conditions and cumulatively resulted in 16.8 ± 0.6 mL $CH_4$ (0.660 ± 0.024 mmol) over 3 d (all volumes reported in this work assume 1-atm pressure and a temperature of 310 K) with an average Faradaic efficiency of 81 ± 3% ($n = 3$). (All errors represent standard deviation unless otherwise noted.) (Fig. 2*B*). Electrolysis was subsequently conducted in rich media containing yeast extract and casitone; variation of the applied current from 1 mA ($j = 0.12$ mA/cm$^2$) to 7.5 mA ($j = 0.88$ mA/cm$^2$) shows that $CH_4$ generation is proportional to applied current, suggesting that the system is operating in a hydrogen-limited regime (Fig. 2*C*). The highest Faradaic efficiency, 86 ± 3%, was observed with an applied current of 2.5 mA ($j = 0.29$ mA/cm$^2$). A slight decrease in Faradaic efficiency was observed at higher current densities. We speculate that increased rates of HER cause $H_2$ to be less effectively delivered to the culture solution with loss to the headspace.

To test the limits of $CH_4$ production of the system, the organisms were electrolyzed at 7.5 mA for 7 d (Fig. 2*D*). The headspace of the cathodic chamber was sampled daily and subsequently exchanged with fresh $CO_2$. During each 24-h period (23 h electrolysis and 1 h sampling), 15.6 ± 0.7 mL $CH_4$ (0.613 ± 0.028 mmol) were produced; this value corresponds to cumulative methane production of 109 ± 5 mL (4.28 ± 0.20 mmol) over 7 d at an average Faradaic efficiency of 75 ± 4% ($n = 3$). Moreover, the hybrid bioinorganic system showed no loss in efficiency over the course of the experiments, which were terminated due to time constraints rather than a decrease in performance. Taken together, these data establish that there are no viability concerns on the timescale tested and presage the possibility of extended operation with a single inoculation of biomass.

A series of isotopic labeling experiments was conducted to show that the observed methane was derived from carbon dioxide. Electrolysis cells containing nitrogen-sparged rich media were inoculated with *M. barkeri*. The headspace of one cell was filled with $^{12}CO_2$ and another with $^{13}CO_2$, and both were subjected to galvanostatic electrolysis at a current of 2.5 mA. High-resolution GC-mass spectrometry was used to show that only $^{13}CH_4$ was observed when electrolyzed under an atmosphere of $^{13}CO_2$ (Fig. 2*F*), whereas only $^{12}CH_4$ was observed in the $^{12}CO_2$ control experiment (Fig. 2*E*). Based on the limit of detection and amount of methane generated, <4% of the observed methane could potentially come from sources other than $CO_2$. Similarly, only $^{13}CH_4$ was observed when the electrolysis was performed in minimal media (Fig. S3). Based on the limit of detection and amount of methane generated, <7.5% of the observed methane could potentially come from sources other than $CO_2$ under these conditions.

**Synthesis and Characterization of α-NiS HER Catalyst and Its Use in Carbon Dioxide to Methane Conversion.** After demonstrating $CO_2$-to-$CH_4$ conversion by *M. barkeri* during in situ electrolysis using a platinum HER cathode, we sought to replace the precious metal catalyst with an earth-abundant alternative. Several HER catalysts containing only first-row transition metals have been recently reported (57–60); among these examples, metal chalcogenides have featured prominently (61–67). In addition to low overpotential and long-term stability, another requirement for a catalyst in a biomaterials hybrid system is that it must operate in aqueous media within a biologically relevant pH range (pH 5–8) and be nontoxic to the organism. Relatively few published examples meet all of these criteria. As such, we developed nanoparticulate α-NiS as a biocompatible HER catalyst for integration with *M. barkeri* cultures.

Nanoparticulate nickel sulfide was prepared by microwave irradiation (250 °C, 30 min) of an aqueous solution of nickel chloride, thioacetamide, and ammonium hydroxide (Fig. 3*A*). The resulting black powder was rinsed with water and isopropanol and dried under vacuum overnight. The newly synthesized catalyst was stored in a capped vial in air and retained activity for several months. Characterization by powder X-ray diffraction (pXRD) confirmed that the product is crystalline and identified the primary phase as α-NiS (Joint Committee on Powder Diffraction Standards number 77–1624) (Fig. 3*B*). Transmission electron microscopy (TEM) images show polydisperse hexagonal particles of 20–100-nm diameter (Fig. S4). The nickel-to-sulfur ratio was verified to be 1:1 by energy-dispersive X-ray (EDX) spectroscopy based on the nickel L and sulfur K peaks (Fig. 3*C*), a result which was further corroborated by inductively coupled plasma-optical emission spectroscopy (ICP-OES) measurements. High-resolution TEM images taken along the [010] axis confirm the assignment of single-crystalline α-NiS based on the (100) and (001) lattice planes (Fig. 3*D*). Thermogravimetric analysis (TGA) shows negligible loss of mass until 600 °C, suggesting the absence of surface-bound organics (Fig. S5).

Electrocatalytic properties of the α-NiS particles were evaluated using rotating disk electrochemistry and chronopotentiometry. As shown in the polarization curve (Fig. 3*E*), crystalline α-NiS is an active HER catalyst in pH 7 potassium phosphate buffer and achieves current densities of 1 and 5 mA/cm$^2$ at overpotentials of $\eta = 275$ and 350 mV, respectively. The observed Tafel slope of 111 mV/dec is similar to the predicted 118 mV/dec for a process in which the Volmer step (formation of an adsorbed H intermediate) is rate-determining (68). The exchange current density, $j_0$, is $3.5 \times 10^{-2}$ mA/cm$^2$ based on extrapolation of the Tafel plot (Fig. 3*F*). These parameters compare favorably to other heterogeneous, first-row transition metal HER catalysts, especially given the ease of synthesis (Table S1).

A suspension of α-NiS powder in 3:1 ethanol:water with Nafion binder was deposited on conductive carbon cloth to

fabricate larger-scale electrodes for hydrogen generation and long-term stability measurements. Galvanostatic experiments at a current of 2.5 mA were run for 23 h; the Faradaic efficiency for hydrogen generation was found to be 95 ± 4% ($n$ = 3) (Fig. S6). As shown in Fig. S7*B*, the potential applied during these experiments does not significantly decay over time, indicating that the catalyst is stable under such conditions.

Having established the efficacy and stability of α-NiS as a catalyst for HER at biologically relevant pH, we sought to interface it with a *M. barkeri* culture for electrochemical methane production. A piece of conductive carbon cloth with 1.4 mg deposited α-NiS catalyst was used as an earth-abundant replacement for platinum. In a galvanostatic experiment at 2.5 mA ($j_{avg}$ = 0.28 mA/cm$^2$, η = 695 mV), 5.1 ± 0.2 mL $CH_4$ (0.20 ± 0.01 mmol) were generated in 24 h, cumulatively generating 15.4 ± 0.8 mL $CH_4$ (0.605 ± 0.031 mmol) over 3 d with an average Faradaic efficiency of 73 ± 5% ($n$ = 3) (Fig. S8). These values are comparable to those obtained for the corresponding platinum experiments. When the current was increased to 7.5 mA ($j_{avg}$ = 0.83 mA/cm$^2$), experiments using α-NiS/C were virtually indistinguishable from Pt in terms of daily and cumulative methane, producing 108 ± 4 mL $CH_4$ (4.24 ± 0.16 mmol) over 7 d with an average Faradaic efficiency of 74 ± 2% ($n$ = 3) (Fig. 3*G*).

**Photoelectrochemical Generation of Methane from Carbon Dioxide.** Having performed electrochemical conversion of $CO_2$ to $CH_4$, we next sought to develop a photoelectrochemical system in which a portion of the potential required for water splitting is contributed by light. Indeed, transforming electrochemical systems to photochemical ones remains challenging. To achieve this goal, we sought to use semiconductor photocathodes coated with a thin-film HER catalyst. The overall performance of such an assembly is determined by a tradeoff between efficient catalysis and light absorption: thicker films confer superior electrocatalytic activity and stability, whereas thinner and more transparent films allow for greater photon capture. Although α-NiS proved effective as an earth-abundant HER electrocatalyst, previously published work from our laboratories on the electrodeposition of a related cobalt sulfide film on planar n$^+$/*p*-Si showed that the current density under illumination drastically diminished as the thickness of the film increased (62). For this reason, we chose to use a nickel–molybdenum alloy, a previously characterized earth-abundant HER catalyst, which has shown favorable performance under photocatalytic conditions despite having a slightly larger overpotential than platinum (69). Photoactive cathodes were prepared by sputtering a thin layer of Ni–Mo alloy atop $TiO_2$-passivated $n^+/p$-Si (Fig. 4*A*). To confirm hydrogen evolution, abiotic galvanostatic experiments at a current of 2.5 mA ($j_{avg}$ = 0.36 mA/cm$^2$) were run for 23 h while illuminating the cathode with 740-nm light (20 mW/cm$^2$); Faradaic efficiencies for $H_2$ were 103 ± 3% (Fig. S6). A light toxicity control experiment with *M. barkeri* showed that methane generation is not affected by illumination at this wavelength (Fig. S9*A*). Biological galvanostatic electrolysis at 2.5 mA with the photocathode (740-nm illumination) generated 17.6 ± 2.1 mL $CH_4$ (0.692 ± 0.083 mmol) with a Faradaic efficiency of 82 ± 10% ($n$ = 3) with only 175-mV overpotential (Fig. 4*B*).

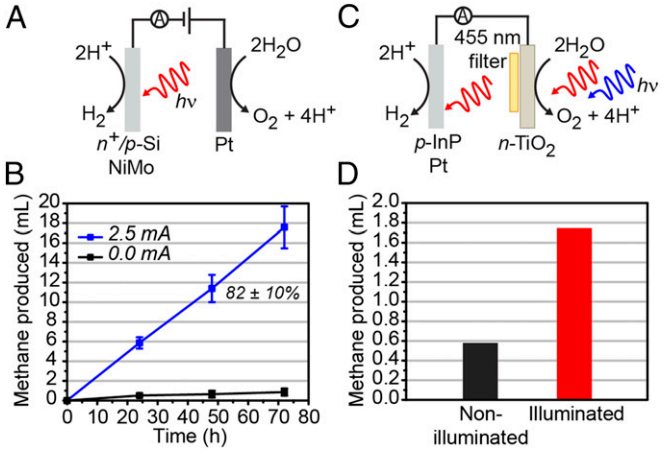


**Fig. 4.** Photoelectrochemical and unassisted solar-driven conversion of carbon dioxide to methane with hybrid bioinorganic catalysts. (*A*) Schematic of electrode setup for photoelectrochemical water splitting. (*B*) Cumulative photoelectrochemically derived methane and associated average Faradaic efficiency with an $n^+/p$-Si/NiMo photocathode illuminated with 740-nm light in rich media. Error bars represent SD with $n$ = 3 independent experiments. (*C*) Schematic of electrode setup for unassisted solar water splitting. (*D*) Average methane produced after 3 d under illuminated ($n$ = 2) and nonilluminated ($n$ = 3) conditions using an $n$-$TiO_2$ photoanode and a *p*-InP/Pt photocathode with no applied potential.

**Unassisted Light-Driven Synthesis of Methane from Carbon Dioxide.** Finally, we sought to construct a fully light-driven hybrid bioinorganic system for $CO_2$-to-$CH_4$ conversion through the use of a tandem semiconductor assembly. In this setup, full-spectrum light first impinges on a large bandgap anode [nanowire $n$-$TiO_2$ on fluorine-doped tin oxide (FTO)], where water oxidation generates oxygen (37). The filtered, lower-energy light subsequently illuminates a smaller bandgap cathode (*p*-InP coated with Pt), where water reduction generates hydrogen (Fig. 4*C*). The electrochemical cell design described above required slight modifications for unassisted photochemical experiments: a 1-in-diameter quartz window was added to the anodic chamber to prevent initial filtering of the full-spectrum light by glass, and the anode and cathode compartments were separated by an anion exchange membrane to minimize pH changes. This linked two-electrode assembly generates nonzero photocurrent under illumination ($i_{avg}$ = 0.17 mA, $j_{avg}$ = 0.057 mA/cm$^2$ during the first hour) (Fig. S7*D*). The Faradaic efficiency for hydrogen generation in abiotic experiments is 100 ± 8% (Fig. S6) ($n$ = 4). Before introduction of *M. barkeri* into such a system, galvanostatic control electrolyses of a *M. barkeri* culture were performed using Pt electrodes under illuminated and nonilluminated conditions. When only the $n$-$TiO_2$/FTO anode was used as a light filter, lower than expected Faradaic efficiencies for methane were observed in the illuminated experiment (Fig. S9*B*); this is in agreement with literature concerning the photosensitivity of methanogenic archaea to blue light (70, 71). Installation of a 455-nm filter directly after the photoanode restored the Faradaic efficiency for methane to expected levels (Fig. S9*B*). Experiments to produce methane using this hybrid bioinorganic system were conducted similarly to those described earlier except headspace analysis was performed only once per experiment after 3 d. On average, 1.75 mL $CH_4$ (68.8 nmol) ($n$ = 2) were produced in illuminated experiments, whereas only 0.58 mL $CH_4$ (22.8 nmol) ($n$ = 3) were produced in identical nonilluminated controls (Fig. 4*D*). We note that higher background levels of methane production were observed in these unassisted photochemical experiments compared with the electrochemical and photoelectrochemical experiments and speculate that this may be due to biological corrosion of the multicomponent photocathode, a phenomenon previously documented in other systems (53, 72). Subtraction of the background methane results in an average Faradaic efficiency of 74%. This result clearly demonstrates the successful conversion of $CO_2$ to $CH_4$ using light as the sole energy input.

## Concluding Remarks

In summary, we have established a hybrid bioinorganic approach to solar-to-chemical conversion by transforming carbon dioxide and water to the value-added chemical product methane. The present integrated system couples inorganic hydrogen generation

catalysts powered by sustainable electrical and/or solar energy inputs with a biological catalyst that can harvest reducing equivalents from $H_2$ to convert carbon dioxide to methane with up to 86% Faradaic efficiency. The data show that the low aqueous solubility and mass transfer rate of hydrogen do not preclude it from being an effective molecular redox carrier and offer a starting platform for potential integration with sustainable sources of electricity (e.g., solar, wind, hydrothermal, nuclear, etc.). Indeed, a solar-to-chemical efficiency of 10% and an electrical-to-chemical efficiency of 52%, which compare favorably to previously reported systems (73), are possible given caveats of materials and biological integration, assuming efficiency values of 20% for solar-to-electrical conversion using a commercially available photovoltaic and 70% for electrical-to-hydrogen conversion in an optimized system (74), as well as 86% energetic efficiency for $H_2$ to $CH_4$ based on thermodynamic values. Furthermore, we have developed an earth-abundant nanoparticulate nickel sulfide HER catalyst that operates effectively under biologically compatible conditions. At an applied current of 7.5 mA, use of the α-NiS catalyst results in 110 mL (4.3 mmol) of methane over 7 d with a Faradaic efficiency of 74%, comparable to Pt. Moreover, we have demonstrated that use of a photoactive silicon cathode results in an overpotential of only 175 mV, allowing for greater methane generation from a defined quantity of electrical energy. Finally, combining an *n*-$TiO_2$ photoanode with a *p*-InP photocathode allows for fully unassisted light-driven conversion of $CO_2$ to $CH_4$. By realizing an effective artificial photosynthesis platform for the production of a value-added chemical product from light, $CO_2$, and water, these results provide a starting point for achieving sustainable chemistry with materials biology.

## Materials and Methods

**Materials.** Reagents were purchased from commercial sources as noted in the *Supporting Information* and used without further purification. Ultrahigh-purity gases purchased from Praxair were used for all anaerobic manipulations. $^{13}$C-labeled $CO_2$ was purchased from Cambridge Isotopes. Distilled water ($dH_2O$) was deionized to a resistivity of 18.2 MΩ·cm using a Millipore Milli-Q UF Plus system ($ddH_2O$).

**Strain Details and Culture Conditions.** *M. barkeri* (ATCC 43241) was purchased from the American Type Culture Collection (ATTC). All culture manipulations were performed inside a Vacuum Atmospheres Nexus One glovebox with an atmosphere of 90% nitrogen and 10% hydrogen. Oxygen levels and humidity levels within the box were controlled using a STAK-PAK palladium catalyst and desiccant system in a Coy Laboratory Products unheated fan box. *M. barkeri* primary cultures were propagated in 18 × 150-mm Balch tubes with butyl rubber stoppers and aluminum crimp seals using ATCC medium 1043 with deoxygenated methanol (1% vol/vol) as the growth substrate. Secondary cultures were started by diluting late exponential phase primary cultures 1:100 into 1 L of ATCC medium 1043 in a 2-L anaerobic media bottle with deoxygenated methanol (1% vol/vol) as the growth substrate. All cultures were grown at 37 °C with shaking (200 rpm). The primary culture was propagated by diluting 1:100 into fresh ATCC 1043 medium every 4 d for ∼3–4 mo, or until changes in growth patterns were observed. Glycerol stocks were used for long-term culture storage.

**General Experimental Setup.** A *M. barkeri* secondary culture was harvested after 4 d of growth by centrifugation at 6,000 × *g* for 7 min at 4 °C using O-ring–sealed centrifuge bottles. After centrifugation, the pellets were combined and washed twice with methanol-free media (200 mL). The final washed pellet was resuspended in fresh methanol-free media (20 mL). At this point, the $OD_{600\ nm}$ of the culture was determined by diluting the cell suspension 1:100 into 10 mM Tris buffer (pH 8.5).

The electrolysis cells were assembled inside an anaerobic glovebox. The appropriate media was added to the cathodic (130 mL) and anodic (70 mL) compartments as specified in the *Supporting Information*. Additionally, a magnetic stirbar was added to the cathodic compartment. The resuspended cell pellet was used to inoculate the cathodic side of the electrolysis cell to a final $OD_{600\ nm}$ of 0.35. Appropriate electrodes were added to the cathodic and anodic compartments, and the tightly sealed electrolysis cells were removed from the anaerobic chamber. Once outside, the cathodic compartment was sparged with $CO_2$ for 5 min using the internal sparge line. Helium (1 mL) was injected into the cathodic headspace as a gaseous internal standard. The electrolysis cells were submerged to the horizontal flanges in water baths set to 37 °C. The cultures were stirred at 300 rpm for the duration of the experiment. In experiments with 24-h (12-h) timepoints, the experimental interval consisted of 23 h (11.5 h) of electrolysis followed by a 1-h (0.5-h) period for headspace analysis and sparging. GC analysis was performed at each timepoint by direct introduction of the headspace into a GC sampling loop as described in the *Supporting Information*. Immediately after sampling, the headspace of the cathodic chamber was exchanged by sparging with fresh $CO_2$ for 5 min via the internal sparge line, followed by injection of a helium (1 mL) internal standard.

**Synthesis of α-NiS Catalyst.** Freshly prepared solutions of $NiCl_2{\cdot}6H_2O$ (0.2 M), thioacetamide (0.4 M), and 5% (vol/vol) ammonium hydroxide were prepared using $ddH_2O$. Nickel chloride solution (2 mL) and thioacetamide solution (2 mL) were combined in a 10-mL microwave reaction vial and sparged with $N_2$ for 10 min. Upon addition of ammonium hydroxide solution (40 μL), a small amount of yellow precipitate was observed. The reaction tube was then capped under $N_2$ and microwaved for 30 min at 150 °C with a 5-min temperature ramp using a CEM microwave reactor. Following the reaction, the supernatant was decanted and the black particles were washed three times with $ddH_2O$ and once with isopropanol by centrifuging the sample, decanting the supernatant, and resuspending the particles. Drying under vacuum overnight yielded a fine black powder (22 mg, 61% yield). The product was characterized by rotating disk electrochemistry (RDE) and galvanostatic experiments, pXRD, EDX, TEM, high-resolution TEM (HRTEM), ICP-OES, and TGA as described in the *Supporting Information*. The catalyst was stored in air for 3–4 mo, after which time it was found to be no longer active for HER.

**Electrochemical Details.** All electrochemical experiments were performed using a BASi Epsilon potentiostat. Pt gauze (electrochemical grade, purchased from Alfa Aesar or Sigma-Aldrich) was used as the anode in all experiments except the unassisted full-splitting, where an *n*-$TiO_2$-coated FTO anode was used instead. The reference electrode was an aqueous Ag/AgCl electrode (3.5 M KCl) purchased from BASi. All reference electrodes were externally calibrated to potassium ferricyanide in pH 7 phosphate buffer ($Fe^{3+/2+}$ couple is 0.436 V vs. standard hydrogen electrode) before and after each experiment. No iR compensation was applied.

**ACKNOWLEDGMENTS.** We thank Dr. Zhongrui Zhou for help with HR GC-MS analysis, Dr. Hans Carlson for helpful advice on methanogen culturing, and Prof. Jonah Jurss for help with the design of electrochemical cells. This work was supported by DOE/LBNL DE-AC02-05CH11231, FWP CH030201 (to C.J.C. and M.C.Y.C.), a Laboratory Directed Research and Development Seed Grant from LBNL (to C.J.C. and M.C.Y.C.), and DOE/LBNL DE-AC02-05CH11231, PChem ( to P.Y.). C.J.C. is an Investigator with the Howard Hughes Medical Institute. E.M.N. and J.J.G. gratefully acknowledge support from the National Science Foundation Graduate Research Fellowship Program (NSF GRFP). J.J.G. also acknowledges support from NIH Training Grant 1 T32 GMO66698. J.R. gratefully acknowledges the support of the NSF GRFP under Grant DGE-0802270, and the University of California, Berkeley Chancellor's fellowship. This work used the Vincent J. Proteomics/Mass Spectrometry Laboratory at University of California, Berkeley, supported in part by NIH S10 Instrumentation Grant S10RR025622.

1. Lewis NS, Nocera DG (2006) Powering the planet: Chemical challenges in solar energy utilization. *Proc Natl Acad Sci USA* 103(43):15729–15735.
2. Gray HB (2009) Powering the planet with solar fuel. *Nat Chem* 1(1):7.
3. Meyer TJ (1989) Chemical approaches to artificial photosynthesis. *Acc Chem Res* 22(5): 163–170.
4. Benson EE, Kubiak CP, Sathrum AJ, Smieja JM (2009) Electrocatalytic and homogeneous approaches to conversion of $CO_2$ to liquid fuels. *Chem Soc Rev* 38(1): 89–99.
5. Morris AJ, Meyer GJ, Fujita E (2009) Molecular approaches to the photocatalytic reduction of carbon dioxide for solar fuels. *Acc Chem Res* 42(12):1983–1994.
6. Finn C, Schnittger S, Yellowlees LJ, Love JB (2012) Molecular approaches to the electrochemical reduction of carbon dioxide. *Chem Commun* 48(10):1392–1399.
7. Appel AM, et al. (2013) Frontiers, opportunities, and challenges in biochemical and chemical catalysis of $CO_2$ fixation. *Chem Rev* 113(8):6621–6658.
8. Costentin C, Robert M, Savéant JM (2013) Catalysis of the electrochemical reduction of carbon dioxide. *Chem Soc Rev* 42(6):2423–2436.
9. Fisher BJ, Eisenberg R (1980) Electrocatalytic reduction of carbon dioxide by using macrocycles of nickel and cobalt. *J Am Chem Soc* 102(24):7361–7363.
10. Hawecker J, Lehn J, Ziessel R (1984) Electrocatalytic reduction of carbon dioxide mediated by Re(bipy)$(CO)_3$Cl (bipy = 2,2′-bipyridine). *J Chem Soc, Chem Commun* 6(6):328–330.

11. Beley M, Collin JP, Ruppert R, Sauvage JP (1986) Electrocatalytic reduction of carbon dioxide by nickel cyclam$^{2+}$ in water: Study of the factors affecting the efficiency and the selectivity of the process. *J Am Chem Soc* 108(24):7461–7467.
12. Bourrez M, Molton F, Chardon-Noblat S, Deronzier A (2011) [Mn(bipyridyl)$(CO)_3$Br]: An abundant metal carbonyl complex as efficient electrocatalyst for $CO_2$ reduction. *Angew Chem Int Ed Engl* 50(42):9903–9906.
13. Schneider J, et al. (2012) Nickel(II) macrocycles: Highly efficient electrocatalysts for the selective reduction of $CO_2$ to CO. *Energy Environ Sci* 5(11):9502–9510.
14. Kang P, Meyer TJ, Brookhart M (2013) Selective electrocatalytic reduction of carbon dioxide to formate by a water-soluble iridium pincer catalyst. *Chem Sci* 4(9):3497–3502.
15. Thoi VS, Kornienko N, Margarit CG, Yang P, Chang CJ (2013) Visible-light photoredox catalysis: Selective reduction of carbon dioxide to carbon monoxide by a nickel N-heterocyclic carbene-isoquinoline complex. *J Am Chem Soc* 135(38):14413–14424.
16. Agarwal J, et al. (2014) NHC-containing manganese(I) electrocatalysts for the two-electron reduction of $CO_2$. *Angew Chem Int Ed Engl* 53(20):5152–5155.
17. Hori Y (2008) Electrochemical $CO_2$ reduction on metal electrodes. *Modern Aspects of Electrochemistry, No. 42*, eds Vayenas CG, White RE, Gamboa-Aldeco ME (Springer, New York), pp 89–189.
18. Kumar B, et al. (2012) Photochemical and photoelectrochemical reduction of $CO_2$. *Annu Rev Phys Chem* 63:541–569.
19. Barton EE, Rampulla DM, Bocarsly AB (2008) Selective solar-driven reduction of $CO_2$ to methanol using a catalyzed p-GaP based photoelectrochemical cell. *J Am Chem Soc* 130(20):6342–6344.
20. Rosen BA, et al. (2011) Ionic liquid-mediated selective conversion of $CO_2$ to CO at low overpotentials. *Science* 334(6056):643–644.
21. Zhu W, et al. (2013) Monodisperse Au nanoparticles for selective electrocatalytic reduction of $CO_2$ to CO. *J Am Chem Soc* 135(45):16833–16836.
22. Kim D, Resasco J, Yu Y, Asiri AM, Yang P (2014) Synergistic geometric and electronic effects for electrochemical reduction of carbon dioxide using gold-copper bimetallic nanoparticles. *Nat Commun* 5:4948.
23. Lu Q, et al. (2014) A selective and efficient electrocatalyst for carbon dioxide reduction. *Nat Commun* 5:3242.
24. Zhang S, et al. (2014) Polyethylenimine-enhanced electrocatalytic reduction of $CO_2$ to formate at nitrogen-doped carbon nanomaterials. *J Am Chem Soc* 136(22):7845–7848.
25. Medina-Ramos J, Pupillo RC, Keane TP, DiMeglio JL, Rosenthal J (2015) Efficient conversion of $CO_2$ to CO using tin and other inexpensive and easily prepared post-transition metal catalysts. *J Am Chem Soc* 137(15):5021–5027.
26. Min X, Kanan MW (2015) Pd-catalyzed electrohydrogenation of carbon dioxide to formate: High mass activity at low overpotential and identification of the deactivation pathway. *J Am Chem Soc* 137(14):4701–4708.
27. Parkinson BA, Weaver PF (1984) Photoelectrochemical pumping of enzymatic $CO_2$ reduction. *Nature* 309(5964):148–149.
28. Shin W, Lee SH, Shin JW, Lee SP, Kim Y (2003) Highly selective electrocatalytic conversion of $CO_2$ to CO at -0.57 V (NHE) by carbon monoxide dehydrogenase from *Moorella thermoacetica*. *J Am Chem Soc* 125(48):14688–14689.
29. Parkin A, Seravalli J, Vincent KA, Ragsdale SW, Armstrong FA (2007) Rapid and efficient electrocatalytic $CO_2$/CO interconversions by *Carboxydothermus hydrogenoformans* CO dehydrogenase I on an electrode. *J Am Chem Soc* 129(34):10328–10329.
30. Reda T, Plugge CM, Abram NJ, Hirst J (2008) Reversible interconversion of carbon dioxide and formate by an electroactive enzyme. *Proc Natl Acad Sci USA* 105(31):10654–10658.
31. Woolerton TW, et al. (2010) Efficient and clean photoreduction of $CO_2$ to CO by enzyme-modified $TiO_2$ nanoparticles using visible light. *J Am Chem Soc* 132(7):2132–2133.
32. Gust D, Moore TA, Moore AL (2001) Mimicking photosynthetic solar energy transduction. *Acc Chem Res* 34(1):40–48.
33. Magnuson A, et al. (2009) Biomimetic and microbial approaches to solar fuel generation. *Acc Chem Res* 42(12):1899–1909.
34. Armstrong FA, Hirst J (2011) Reversibility and efficiency in electrocatalytic energy conversion and lessons from enzymes. *Proc Natl Acad Sci USA* 108(34):14049–14054.
35. Braun A, et al. (2015) Biological components and bioelectronic interfaces of water splitting photoelectrodes for solar hydrogen production. *Chemistry* 21(11):4188–4199.
36. Liu C, et al. (2015) Nanowire-bacteria hybrids for unassisted solar carbon dioxide fixation to value-added chemicals. *Nano Lett* 15(5):3634–3639.
37. Liu C, Tang J, Chen HM, Liu B, Yang P (2013) A fully integrated nanosystem of semiconductor nanowires for direct solar water splitting. *Nano Lett* 13(6):2989–2992.
38. Nevin KP, Woodard TL, Franks AE, Summers ZM, Lovley DR (2010) Microbial electrosynthesis: Feeding microbes electricity to convert carbon dioxide and water to multicarbon extracellular organic compounds. *MBio* 1(2):e00103–e00110.
39. Rabaey K, Rozendal RA (2010) Microbial electrosynthesis - revisiting the electrical route for microbial production. *Nat Rev Microbiol* 8(10):706–716.
40. Lovley DR, Nevin KP (2013) Electrobiocommodities: Powering microbial production of fuels and commodity chemicals from carbon dioxide with electricity. *Curr Opin Biotechnol* 24(3):385–390.
41. Li H, et al. (2012) Integrated electromicrobial conversion of $CO_2$ to higher alcohols. *Science* 335(6076):1596.
42. Torella JP, et al. (2015) Efficient solar-to-fuels production from a hybrid microbial-water-splitting catalyst system. *Proc Natl Acad Sci USA* 112(8):2337–2342.
43. Hori Y, Takahashi I, Koga O, Hoshi N (2002) Selective formation of C2 compounds from electrochemical reduction of $CO_2$ at a series of copper single crystal electrodes. *J Phys Chem B* 106(1):15–17.
44. Manthiram K, Beberwyck BJ, Alivisatos AP (2014) Enhanced electrochemical methanation of carbon dioxide with a dispersible nanoscale copper catalyst. *J Am Chem Soc* 136(38):13319–13325.
45. Meng X, et al. (2014) Photothermal conversion of $CO_2$ into $CH_4$ with $H_2$ over Group VIII nanocatalysts: An alternative approach for solar fuel production. *Angew Chem Int Ed Engl* 53(43):11478–11482.
46. Thauer RK (1998) Biochemistry of methanogenesis: A tribute to Marjory Stephenson. 1998 Marjory Stephenson Prize Lecture. *Microbiology* 144(Pt 9):2377–2406.
47. Anbarasan P, et al. (2012) Integration of chemical catalysis with extractive fermentation to produce fuels. *Nature* 491(7423):235–239.
48. Sirasani G, Tong L, Balskus EP (2014) A biocompatible alkene hydrogenation merges organic synthesis with microbial metabolism. *Angew Chem Int Ed Engl* 53(30):7785–7788.
49. Schlegel HG, Lafferty R (1965) Growth of "Knallgas" bacteria (*Hydrogenomonas*) using direct electrolysis of the culture medium. *Nature* 205(4968):308–309.
50. Song J, et al. (2011) Microbes as electrochemical $CO_2$ conversion catalysts. *ChemSusChem* 4(5):587–590.
51. Cheng S, Xing D, Call DF, Logan BE (2009) Direct biological conversion of electrical current into methane by electromethanogenesis. *Environ Sci Technol* 43(10):3953–3958.
52. Van Eerten-Jansen MC, et al. (2013) Microbial community analysis of a methane-producing biocathode in a bioelectrochemical system. *Archaea* 2013:481784.
53. Siegert M, et al. (2014) Comparison of nonprecious metal cathode materials for methane production by electromethanogenesis. *ACS Sustain Chem Eng* 2(4):910–917.
54. Fast AG, Papoutsakis ET (2012) Stoichiometric and energetic analyses of non-photosynthetic $CO_2$-fixation pathways to support synthetic biology strategies for production of fuels and chemicals. *Curr Opin Chem Eng* 1(4):380–395.
55. Mah RA, Smith MR, Baresi L (1978) Studies on an acetate-fermenting strain of *Methanosarcina*. *Appl Environ Microbiol* 35(6):1174–1184.
56. Villano M, et al. (2010) Bioelectrochemical reduction of $CO_2$ to $CH_4$ via direct and indirect extracellular electron transfer by a hydrogenophilic methanogenic culture. *Bioresour Technol* 101(9):3085–3090.
57. Cobo S, et al. (2012) A Janus cobalt-based catalytic material for electro-splitting of water. *Nat Mater* 11(9):802–807.
58. Callejas JF, et al. (2014) Electrocatalytic and photocatalytic hydrogen production from acidic and neutral-pH aqueous solutions using iron phosphide nanoparticles. *ACS Nano* 8(11):11101–11107.
59. Gong M, et al. (2014) Nanoscale nickel oxide/nickel heterostructures for active hydrogen evolution electrocatalysis. *Nat Commun* 5:4695.
60. Jiang N, You B, Sheng M, Sun Y (2015) Electrodeposited cobalt-phosphorous-derived films as competent bifunctional catalysts for overall water splitting. *Angew Chem Int Ed Engl* 54(21):6251–6254.
61. Kong D, Cha JJ, Wang H, Lee HR, Cui Y (2013) First-row transition metal dichalcogenide catalysts for hydrogen evolution reaction. *Energy Environ Sci* 6(12):3553–3558.
62. Sun Y, et al. (2013) Electrodeposited cobalt-sulfide catalyst for electrochemical and photoelectrochemical hydrogen generation from water. *J Am Chem Soc* 135(47):17699–17702.
63. Di Giovanni C, et al. (2014) Bioinspired iron sulfide nanoparticles for cheap and long-lived electrocatalytic molecular hydrogen evolution in neutral water. *ACS Catal* 4(2):681–687.
64. Jiang N, et al. (2014) Electrodeposited nickel-sulfide films as competent hydrogen evolution catalysts in neutral water. *J Mater Chem A* 2(45):19407–19414.
65. Feng LL, et al. (2015) Carbon-armored $Co_9S_8$ nanoparticles as all-pH efficient and durable $H_2$-evolving electrocatalysts. *ACS Appl Mater Interfaces* 7(1):980–988.
66. Tang C, et al. (2015) $Ni_3S_2$ nanosheets array supported on Ni foam: A novel efficient three-dimensional hydrogen-evolving electrocatalyst in both neutral and basic solutions. *Int J Hydrogen Energy* 40(14):4727–4732.
67. Tang C, Pu Z, Liu Q, Asiri AM, Sun X (2015) $NiS_2$ nanosheets array grown on carbon cloth as an efficient 3D hydrogen evolution cathode. *Electrochim Acta* 153:508–514.
68. Conway BE, Tilak BV (2002) Interfacial processes involving electrocatalytic evolution and oxidation of $H_2$, and the role of chemisorbed H. *Electrochim Acta* 47(22-23):3571–3594.
69. McKone JR, Marinescu SC, Brunschwig BS, Winkler JR, Gray HB (2014) Earth-abundant hydrogen evolution electrocatalysts. *Chem Sci* 5(3):865–878.
70. Olson KD, McMahon CW, Wolfe RS (1991) Light sensitivity of methanogenic archaebacteria. *Appl Environ Microbiol* 57(9):2683–2686.
71. Lyon EJ, et al. (2004) UV-A/blue-light inactivation of the "metal-free" hydrogenase (Hmd) from methanogenic archaea. *Eur J Biochem* 271(1):195–204.
72. Daniels L, Belay N, Rajagopal BS, Weimer PJ (1987) Bacterial methanogenesis and growth from $CO_2$ with elemental iron as the sole source of electrons. *Science* 237(4814):509–511.
73. Jhong H, Ma S, Kenis PJ (2013) Electrochemical conversion of $CO_2$ to useful chemicals: Current status, remaining challenges, and future opportunities. *Curr Opin Chem Eng* 2(2):191–199.
74. Zeng K, Zhang D (2010) Recent progress in alkaline water electrolysis for hydrogen production and applications. *Prog Energy Combust Sci* 36(3):307–326.
75. Liu B, Aydil ES (2009) Growth of oriented single-crystalline rutile $TiO_2$ nanorods on transparent conducting substrates for dye-sensitized solar cells. *J Am Chem Soc* 131(11):3985–3990.